

Supplementary Materials

Extrinsic ion migration in perovskite solar cells

Zhen Li,¹ Chuanxiao Xiao,^{1, 2} Ye Yang,¹ Steve Harvey,¹ Dong Hoe Kim,¹ Jeffrey A. Christians,¹ Mengjin Yang,¹ Philip Schulz,¹ Sanjini U. Nanayakkara,¹ Chun-Sheng Jiang,¹ Joseph M. Luther,¹ Joseph Berry,¹ Matthew C. Beard,¹ Mowafak M. Al-Jassim,¹ Kai Zhu^{1,*}

1. National Renewable Energy Laboratory, Golden, Colorado 80401, USA
2. Colorado School of Mines, Golden, CO 80401, USA

Experimental procedures

Synthesis of spiro(TFSI)₂: Synthesis of the pre-oxidized form of 2,2',7,7'-tetrakis(N,N'-di-p-methoxyphenylamine)-9,9'-spirobifluorene (spiro-OMeTAD) followed the procedure described in a previous report.^[1] Briefly, 2.5 g of spiro-OmeTAD (Lumtec) and 1.7 g of silver bis(trifluoromethanesulfonyl)imide (Sigma-Aldrich) were added in 250 mL of dichloromethane and stirred in a nitrogen-filled flask for 24 h. The reaction was dissolved in methylene chloride. The solution was filtered and rotary evaporated leaving a dark black solid. The collected powder was purified by dissolving in dichloromethane and recrystallized in dry diethyl ether. Finally, the black spiro(TFSI)₂ powder was dried under vacuum.

Spiro-OMeTAD doping. Li-free spiro-OMeTAD was prepared by mixing 76 mg of pristine spiro-OMeTAD and 4 mg of spiro(TFSI)₂ (5 wt% pre-oxidized spiro) in 1 mL of chlorobenzene with an additional 32 μ L of 4-tert-butylpyridine (tBP). For Li-doped spiro-OMeTAD, different Li⁺ doping was achieved by adding 2.5, 5, or 10 mg of Li-TFSI (equivalent to Li⁺/spiro mole ratio of 0.13, 0.27, or 0.54) into 1 mL of the above-oxidized Li-free spiro-OMeTAD solution (via 500 mg/mL Li-TFSI acetonitrile solution). Na-doped spiro-OMeTAD was prepared by adding 10.56 mg of Na-TFSI into 1 mL of oxidized Li-free spiro-OMeTAD, with a Na⁺/spiro mole ratio of 0.54 (equivalent to Li⁺/spiro in the 10 mg/mL Li-doped spiro-OMeTAD). H⁺ doping was realized by adding 3.5 μ mol in oxidized Li-free spiro-OMeTAD. The mole ratio of H⁺/spiro is lower than Li⁺/spiro because high H⁺ concentration had a detrimental effect on cell performance.

Solar Cell Fabrication. 20~30 nm TiO₂ compact layer was deposited on patterned fluorine-doped tin oxide (FTO) glass by spray pyrolysis at 450 °C. 50~80 nm TiO₂ nanoparticle layer was deposited by spin coating to block potential pinholes in the TiO₂ compact layer. A perovskite absorber layer was deposited following a “triple-cation” recipe.^[2] The organic halides were purchased from Dyesol; PbI₂ (99.9985%) was purchased from Alfa Aesar; CsI and PbBr₂ (99.999%) were purchased from Sigma-Aldrich. The perovskite precursor solutions contained FAI (1 M), PbI₂ (1.1 M), MABr (0.2 M), and PbBr₂ (0.2 M) in anhydrous DMF:DMSO 4:1 (v:v). 40 μL of 1.5 M CsI stock solution in DMSO was added to the above mixed perovskite precursor. Perovskite films were deposited with spin coating of 1,000 rpm for 10 s and 4,000 rpm for 30 s. 1 mL of toluene was dropped on the spinning substrates at 25 s of the second spin step. After spin-coating, the substrates were annealed at 100 °C for 30 min. Spiro-OMeTAD was spin-coated on the perovskite layer at 4,000 rpm for 30 s. The device was finished after deposition of a 100-nm Au electrode using thermal evaporation.

Time-of-Flight Secondary-Ion Mass Spectrometry (TOF-SIMS). A TOF-SIMS (ION-TOF TOF-SIMS V) was used to depth-profile the perovskite materials and completed devices. Analysis was completed using a 3-lens 30-kV Bi-Mn primary ion gun, the Bi⁺ primary-ion beam (operated in bunched mode; 10-ns pulse width, analysis current of 1.0 pA) was scanned over a 25×25-μm area. Depth profiling was accomplished with a 1-kV oxygen-ion sputter beam (10.8-nA sputter current) raster of 150×150 μm area. All spectra during profiling were collected at a primary ion dose density of 1×10¹² ions/cm² to remain at the static-SIMS limit.

Solar Cell Current Density-Current (J-V) Measurement. Solar cell performance was measured under a simulated AM 1.5G illumination (100 mW/cm², Oriel Sol3A Class AAA Solar Simulator). The light J-V characteristics were measured using a Keithley 2400 source meter with voltage step width of 20 mV; scan rate was controlled by changing the delay time between each step. The step bias and pre-bias J-V curves were measured using a potential station (Princeton Applied Research, VersaSTAT MC) with programmable voltage control.

HTL Resistivity Measurement. The resistivity of the hole-transport layer (HTL) was measured using a 4-wire configuration. Glass substrates were cleaned with acetone and ethanol and treated with UV-Ozone for 20 min. HTLs with different dopants were deposited on the glass substrates with spin coating of 4,000 rpm for 30 s. A parallel four-finger electrode with spacing of 100 μm

was deposited. The resistance was measured using a Keithley 2400 source meter. Thickness of the HTL was measured using a surface profiler.

Time-Resolved Photoluminescence (TRPL). The excitation pulses of TRPL were provided by a Fianium supercontinuum laser. The laser was operating in 0.1-MHz pulse repetition rate, and output wavelength was centered at 600 nm. The photoluminescence (PL) of the samples were focused into a spectrograph (Princeton Instruments, Model SP-2300i) in front of a Streak camera (Hamamatsu universal streak camera C10910). A 650-nm long-pass filter was placed before the entrance of the spectrograph to remove the excitation light. The PL was dispersed by the spectrograph and detected by the streak camera (650–900 nm). The TRPL kinetic traces are obtained by averaging PL kinetics near emission peak (750–770 nm). The time window was set as 5 μ s, and the corresponding temporal width of the instrument response function was determined as 0.15 μ s. Li-TFSI acetonitrile solution was added in the perovskite precursors with Li⁺/Pb²⁺ molar ratio of 0.5% to deposit the Li-doped perovskite thin films (elemental distribution shown in Figure S4). Li-doped PMMA was attained by adding Li-TFSI acetonitrile solution into 10-mg/mL PMMA toluene solution until precipitation. The resulting dispersion was filtered before use. Li doping of TiO₂ was accomplished by spin coating a 0.1 M solution of Li-TFSI in acetonitrile at 4,000 rpm for 30 s. After the spin coating, the substrates were immediately transferred to a hot plate for calcination at 450 °C for 30 min.^[3]

Incident Photon to Current Efficiency (IPCE). IPCE spectra of solar cells were measured using a solar cell quantum-efficiency measurement system (QEX10, PV Measurements). IPCE spectra were measured with a 10-nm step and 10-Hz AC modulation. Each measurement takes about 2 min. The pre-bias measurement was done by applying the external bias in dark for 5 min and measuring the IPCE spectrum from 300 to 850 nm under 0 V bias.

Kelvin Probe Force Microscope (KPFM). KPFM was performed in an Ar-filled glove box with water/oxygen content <0.1 ppm on a Veeco D5000 AFM equipped with the Nanoscope V controller. KPFM measures the contact potential difference between the probe (Nanosensor PPP-EFM) and sample by probing and nullifying the Coulomb force between the probe and sample. Topographic and potential images were collected simultaneously during the probe scanning. We cleaved the devices to expose the cross section without any further treatment (e.g., polishing, ion milling) to the sample. To eliminate the “cross-talk” of topography and electrical potential

signals, the KPFM was conducted on a flat cross-sectional area (<50-nm corrugation). SEM images were taken to identify the interfaces between different layers in the cross section, which was carefully aligned with the AFM images along with potential images. KPFM measurements were performed under different bias voltage from -1.5 V to +1.5 V on the same area. The line profiles were averaged from 32 scan lines of the potential images; each potential image takes about 30 s to capture the transient potential change and continuous mode was used to record the potential revolution until there is no observable change, whereas the analyzed area always remains at the same region. The surface charge on the analyzed area should be fixed during the measurement. Therefore, the evolution of surface potential change in **Figure 5a,b** reflected the potential change in the bulk.^[4]

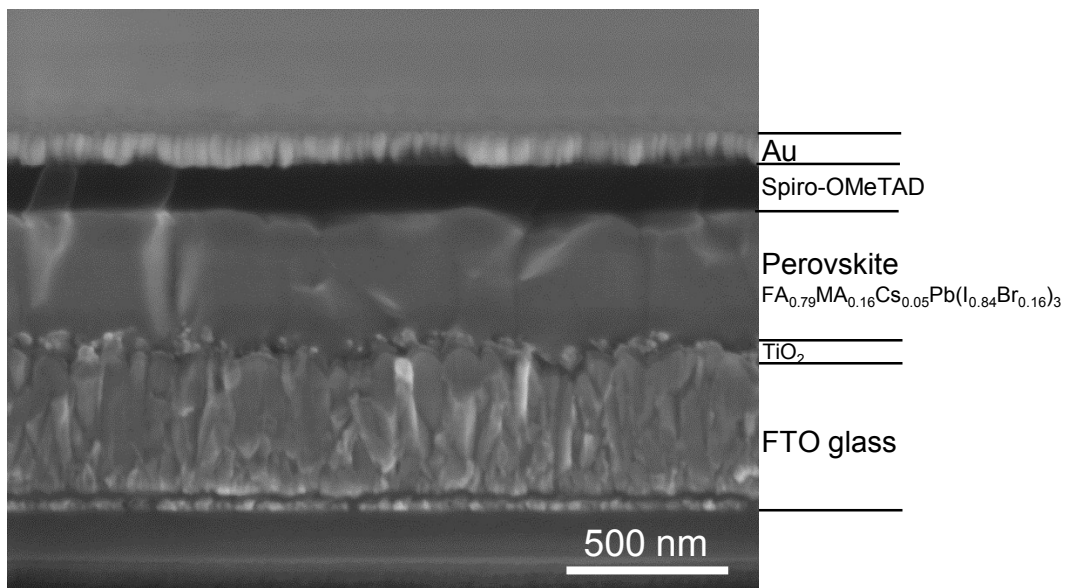


Figure S1. Typical cross-sectional SEM image of a perovskite solar cell. Each layer of the device stack is labeled.

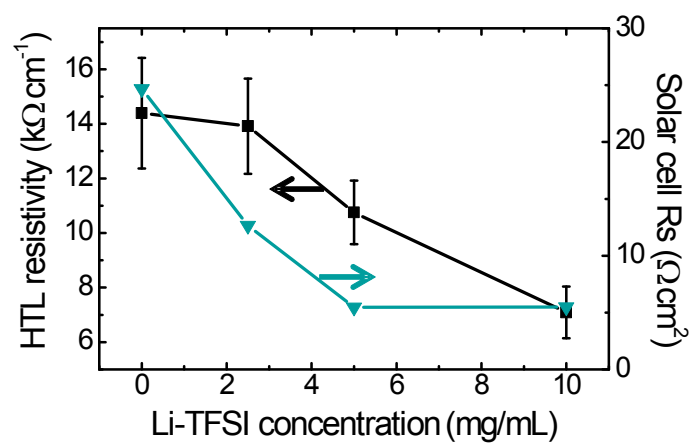


Figure S2. HTL resistivity and solar cell series resistance (R_s) versus Li-TFSI concentration.

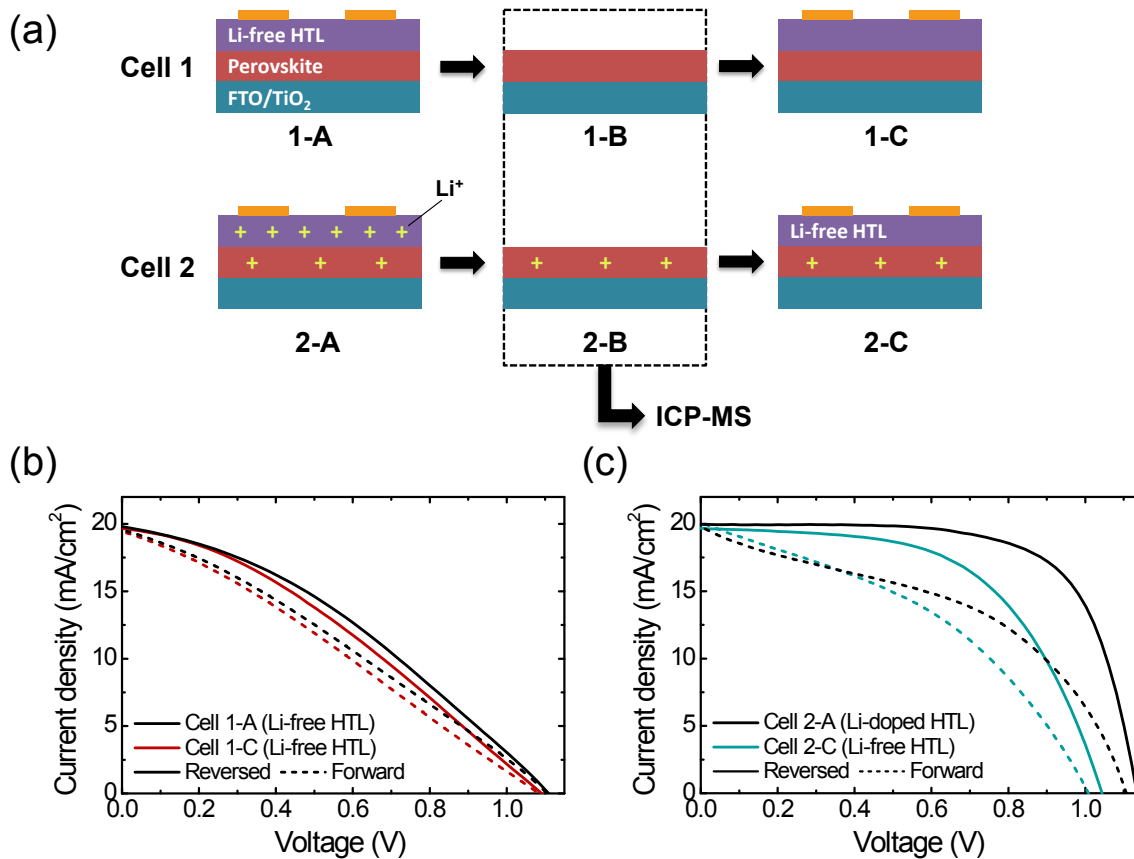


Figure S3. (a) Schematics of removing and redepositing HTL and electrode; (b) Performance change of solar cell with both with Li-free HTL initially (1-A) and finally (1-C), showing negligible efficiency change; (c) Performance change of solar cell with initially Li-doped HTL (2-A) then Li-free HTL (2-C), showing effects of residual Li⁺ in the solar cell.

Table S1. ICP-MS elemental analysis of solar cell absorbers after removing the HTLs

HTL	⁷ Li concentration (ppb)	²⁰⁶ Pb concentration (ppb)	Li/Pb ratio
Li-free	<0.008*	4030.86	<2×10 ⁻⁶
Li-doped	3.19	5029.49	6.7×10 ⁻⁴

* close to the detection limit of the equipment.

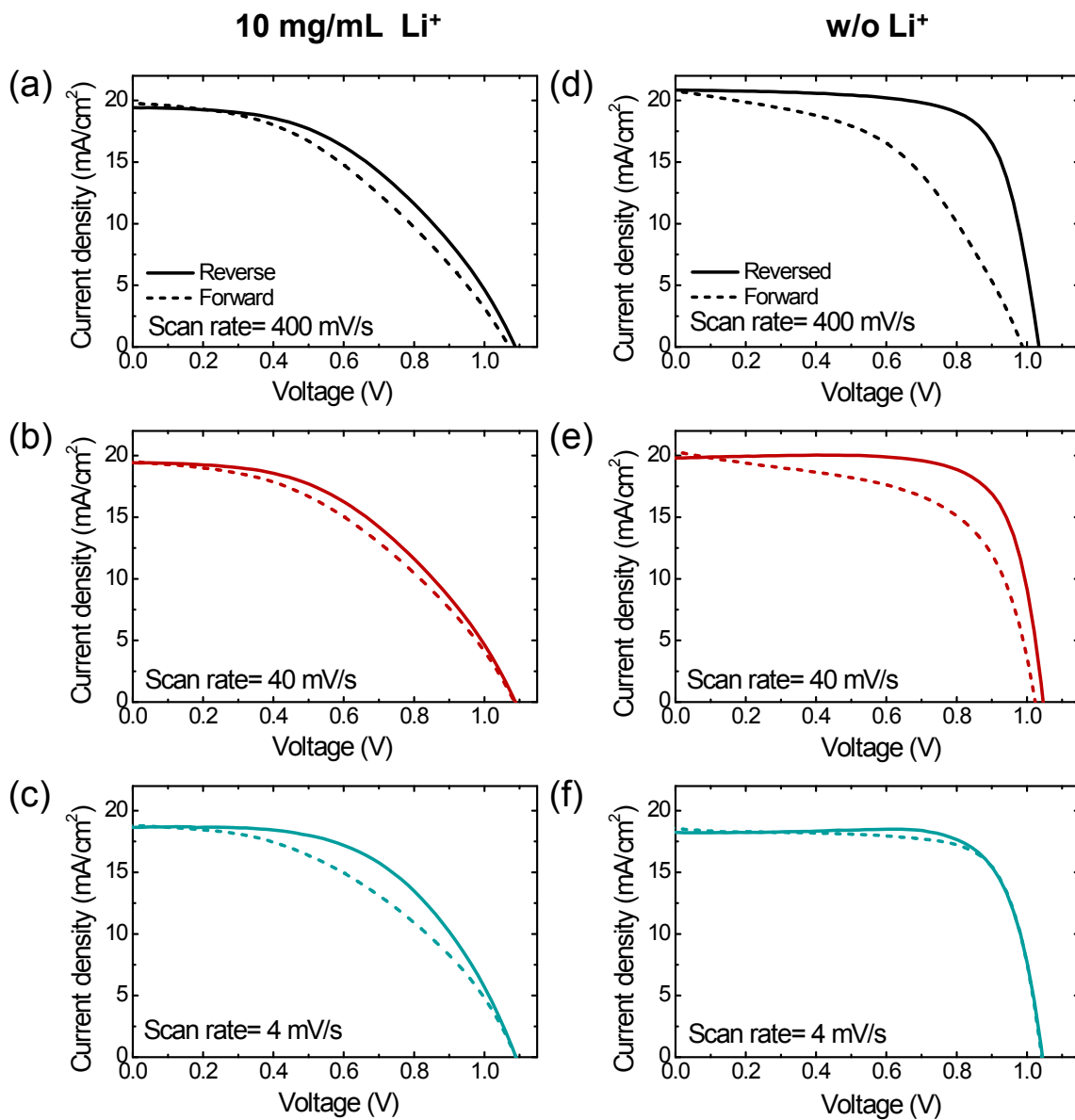


Figure S4. Reverse and forward scan with different scan rate: (a–c) solar cell with Li-doped HTL (10 mg/mL); (d–f) solar cell with Li-free HTL.

Table S2. TRPL lifetime of perovskite with different layer-stacking configurations

Sample index	Layer configurations	Lifetime (μs)
1	Perovskite/PMMA	3.4 ± 0.5
2	Compact TiO_2 /perovskite/PMMA	2.8 ± 0.2
3	Li-doped-perovskite/PMMA	3.9 ± 0.5
4	TiO_2 /Li-doped-perovskite/PMMA	2.02 ± 0.06
5	TiO_2 /perovskite/Li-doped-PMMA	1.97 ± 0.05
6	Li-doped- TiO_2 /perovskite/PMMA	1.37 ± 0.02

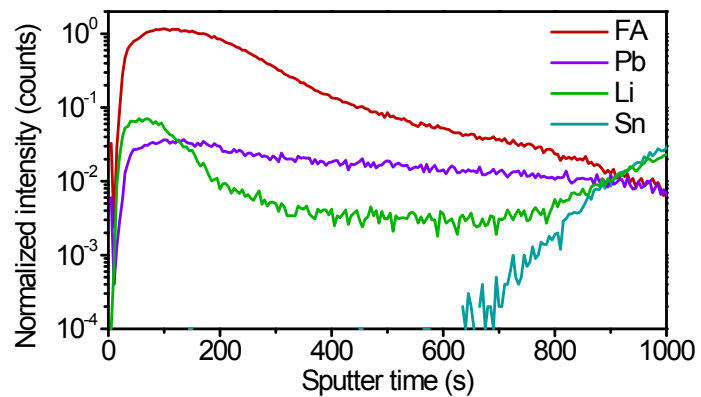


Figure S5. TOF-SIMS element analysis of a typical Li-doped perovskite thin film on FTO glass.

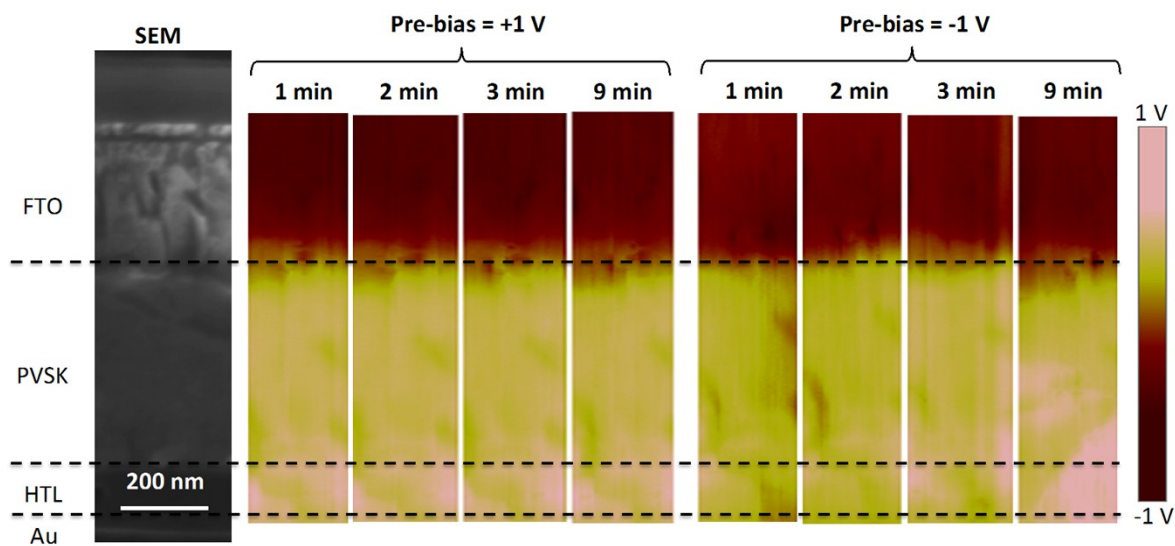


Figure S6. Cross-section and potential images of the PSC with Li-doped HTL. The potential profiles averaged from the images are displayed in **Figure 5a,b**.

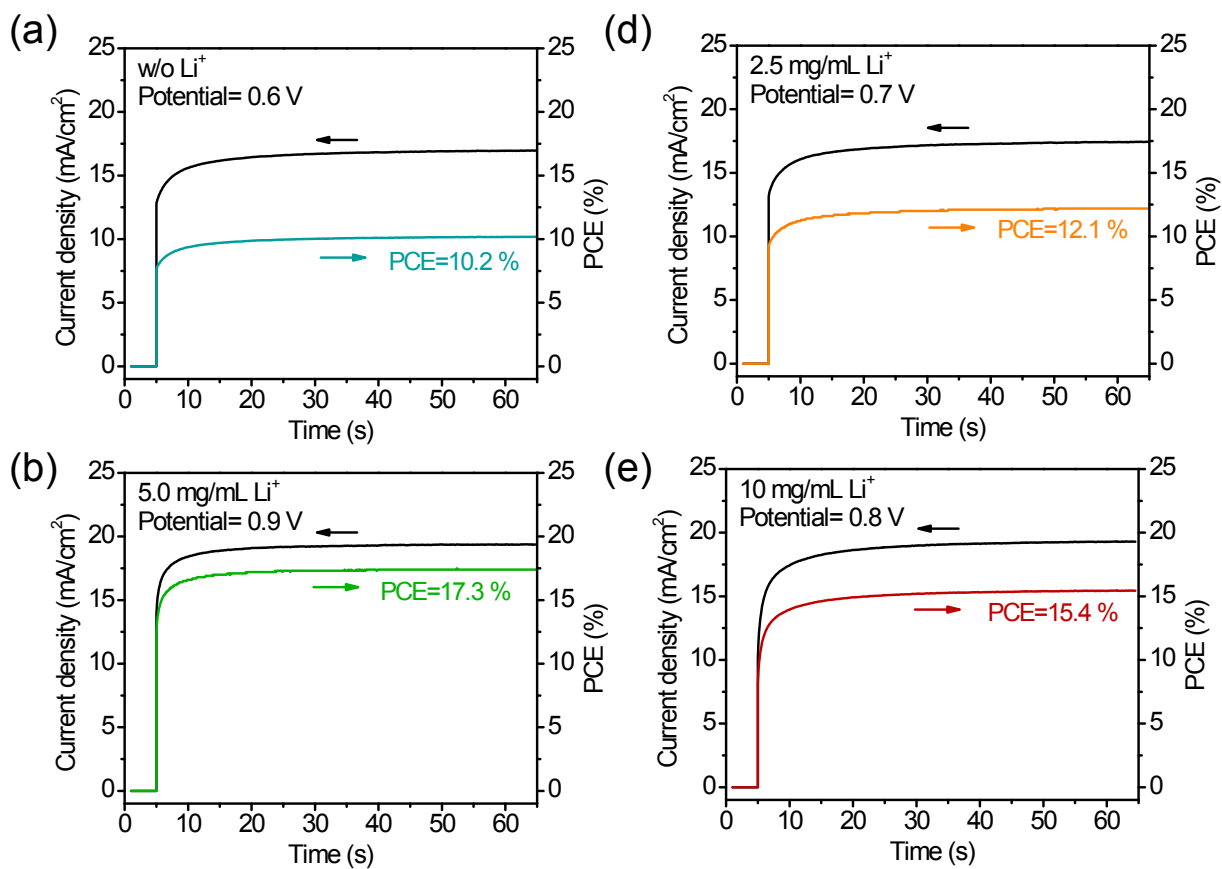


Figure S7. Stable power output of perovskite solar cells with different amount of Li-TFSI in spiro-OMeTAD HTLs.

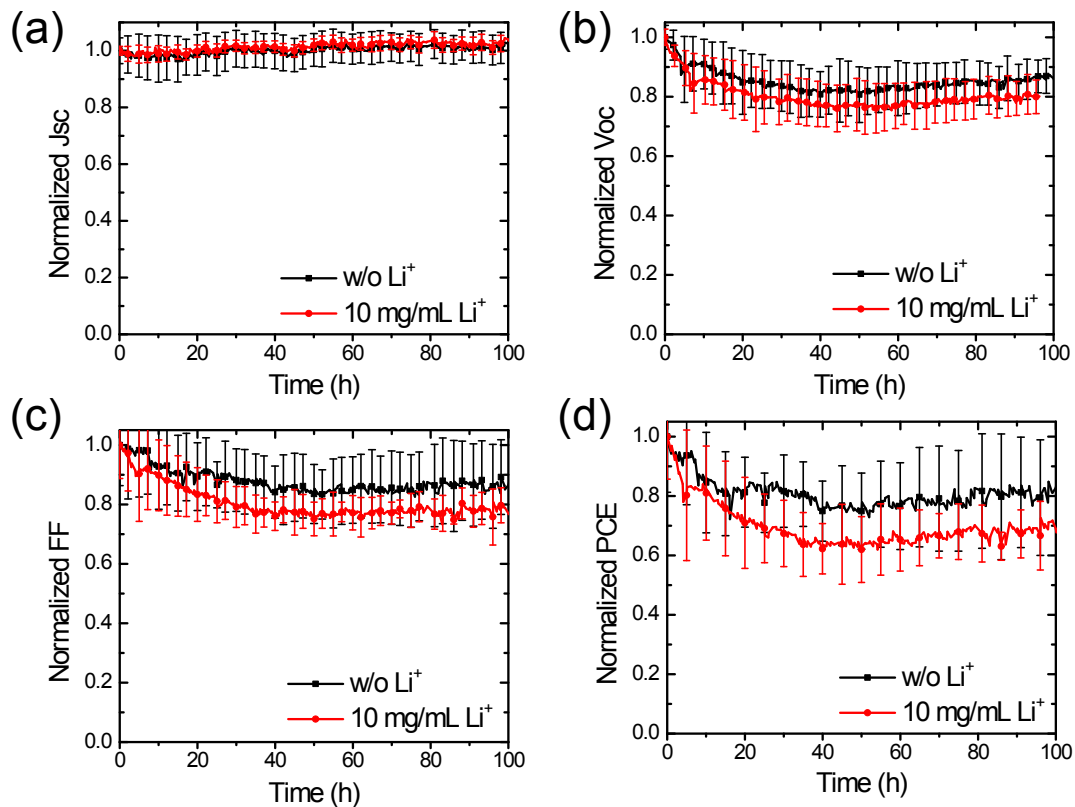


Figure S8. Stability of PSCs with and without Li-TFSI dopants in spiro-OMeTAD. The cells were tested under constant illumination (~ 0.6 sun) in N_2 environment to avoid moisture-induced degradation. The devices were tested every 30 min for 100 hours. The average and standard deviation of the PV parameters from five devices of each type are shown for comparison.

References

- 1 W. H. Nguyen, C. D. Bailie, E. L. Unger and M. D. McGehee, *J. Am. Chem. Soc.*, 2014, **136**, 10996-11001.
- 2 M. Saliba, T. Matsui, J.-Y. Seo, K. Domanski, J.-P. Correa-Baena, M. K. Nazeeruddin, S. M. Zakeeruddin, W. Tress, A. Abate, A. Hagfeldt and M. Gratzel, *Energy Environ. Sci.*, 2016, **9**, 1989-1997.
- 3 F. Giordano, A. Abate, J. P. Correa Baena, M. Saliba, T. Matsui, S. H. Im, S. M. Zakeeruddin, M. K. Nazeeruddin, A. Hagfeldt and M. Gratzel, *Nat Commun*, 2016, **7**, 10379.
- 4 C.-S. Jiang, M. Yang, Y. Zhou, B. To, S. U. Nanayakkara, J. M. Luther, W. Zhou, J. J. Berry, J. van de Lagemaat, N. P. Padture, K. Zhu and M. M. Al-Jassim, *Nat. Commun.*, 2015, **6**, 8397.